A study on shrinkage residual stresses, microstructure and mechanical properties of ASS thick pipe welded by GMAW process

Materials Research Express

PAPER

A study on shrinkage residual stresses, microstructure and mechanical properties of ASS thick pipe welded by GMAW process

Sudhir Kumar[1,*], **Nikki Archana Barla**[2], **Ramkishor Anant**[3] **and Kuldeep Kumar Saxena**[4]

[1] School of Engineering and Technology, Central University of Haryana,123031, India
[2] Metallurgical and Materials Engineering Department, National Institute of Technology, Raipur- 492010, India
[3] Materials and Metallurgical Engineering Department, Maulana Azad National Institute of Technology, Bhopal, India
[4] Department of Mechanical Engineering, GLA University, Mathura, UP, 281406, India
[*] Author to whom any correspondence should be addressed.

E-mail: iitsudhir@gmail.com

Keywords: GMAW process, microstructure, hardness, narrow groove, transverse shrinkage stresses

OPEN ACCESS

RECEIVED
30 August 2021

REVISED
18 October 2021

ACCEPTED FOR PUBLICATION
27 October 2021

PUBLISHED
10 November 2021

Abstract

In this investigation, AISI 304LN austenitic stainless steel pipes having 25 mm thickness and 300 mm inner diameter with conventional and narrow groove were welded by continuous current gas metal arc welding (GMAW) and pulse current gas metal arc welding (P-GMAW) process. A gas tungsten arc welding (GTAW) process was used for the welding of the root pass. Microstructural study was carried out in fusion zone (FZ) and heat-affected zone (HAZ). A favourable microstructure characteristic was observed in the P-GMAW process. The study of transverse shrinkage and shrinkage stresses were done on the conventional groove with GMAW and P-GMAW process and narrow groove by P-GMAW process. It was found that narrow groove weld design with controlled welding parameters can reduce 45% shrinkage as compare to conventional groove, similarly 30% reduction in shrinkage stress can be achieved. The tensile properties were observed to increased, such as yield strength was improved from 260 MPa to 310 MPa and ultimate strength was improved from 510 MPa to 550 MPa in the case of narrow groove weld by the P-GMAW process.

1. Introduction

Austenitic Stainless Steel (ASS) pipe having a significant attraction to industries for various advanced structures like nuclear and thermal power plants, transmission pipelines of oil and gas, industrial equipment, storage tanks, mine and railroad cars and offshore structure etc [1, 2]. The composition of ASS pipe contains chromium 16%–26%, nickel and magnesium 8%–24%, carbon generally below 0.15% and few alloying elements such as Mo, N, Ti, Nb (Cb) and Ta in a small amount [3, 4]. These alloying elements can alter the mechanical and chemical properties of ASS at low as well high temperature [5].

The ASS has excellent resistance to oxidation observed in applications such as boilers, nuclear reactors etc, in which work or process requires compatible strength at high elevated temperature solid solution and particle strengthening mechanisms. Solid solution strengthening in ASS is accomplished by the addition of alloying elements such as titanium, vanadium, niobium, nitrogen, molybdenum etc Depending on alloy addition, ASS alloys are divided into 300 and 200 series, respectively, according to the American Iron and Steel Institute (AISI) system. In Types 304LN and 316LN, extra-low carbon content (0.030% maximum) and a nitrogen range of 0.1 to 0.16% minimizes the precipitation of chromium carbide during welding and controls the sensitizing during post-weld heat treatment [6].

Different welding processes were used to weld ASS. In GMAW, continuous weld metal deposition and automation can be attained. Gas tungsten arc welding (GTAW) process is generally used for root pass welding. In thick pipe welding, multi-pass welding is used [7–9].

Welding processes are associated with thermal cycles, which result in thermal straining due to the contraction of weld and neighbouring base material. Due to this, it generates thermal stresses in weldment and adjacent base material. It harms the performance of weld and its properties like tensile, compressive, hardness and other properties. There is more weld metal deposition in thick pipe or plate welding, so more heat required leads to

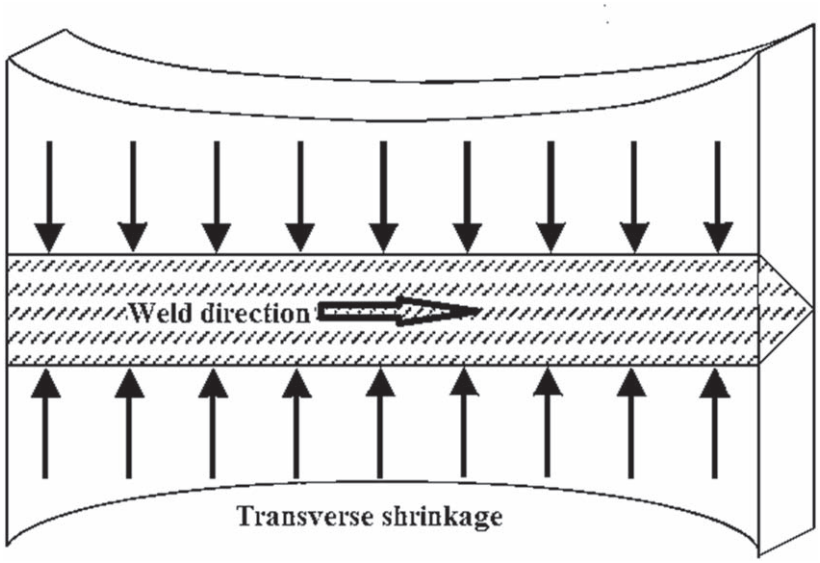

Figure 1. Schematic diagram of transverse shrinkage in a pipe weld.

Table 1. Chemical composition of AISI 304LN.

	Chemical analysis (Wt%)									
Material	C	Cr	Ni	Mn	N	Mo	Si	Cu	S	P
Base metal (304LN)	0.035	19.6	10	2.0	0.14	—	0.75	—	0.03	0.04

complex higher stresses in the weld [10]. The thermal strains are produced in transverse to weld direction. In the GMAW process, there is a continuous heat supply, and the P-GMAW method is preferred in which pulsed current is used. A constant amount of argon in both the GMAW and P-GMAW processes is utilized as the shielding gas [11].

P-GMAW process heat the workpiece comparatively less severely depending on the pulse parameters, which improves the fusion of the weld. The appropriate pulse parameters selection through controlled thermal and metal transfer behaviour depending on the weld pool droplet become relatively complicated due to simultaneous influence of the pulse parameters such as peak current (I_p), base current (I_b), pulse time (t_p) on each other at a given mean current (I_m) of P-GMAW process [12–14].

In the present investigation, both GMAW and P-GMAW processes were used for thick ASS pipes for comparing the residual shrinkages and shrinkage stresses. The welding parameters were selected based on individual pipe weld groove geometries. Conventional and narrow grooved weld were used for the study [15].

Transverse shrinkage is in the perpendicular direction to the weld direction, as shown in figure 1. It is developed due to high localized heating and cooling of material, therefore the shrinkage is generated in the pipe or plate. These stresses are controlled by controlling the weld area, heat input, welding procedure etc.

Transverse shrinkage stresses are measure by the following formula.

$$\sigma_{tr(i-j)} = \frac{\Delta}{N} \times \frac{a}{h} \times \frac{E}{Ls} \quad (1)$$

Transverse shrinkage stress (MPa) denoted by 'σ_{tr}', transverse shrinkage (mm) denoted by 'Δ', number of weld layer denoted by 'N', Modulus of elasticity (GPa) denoted by 'E' (200 GPa), straining length (mm) denoted by 'Ls', wall thickness of pipe (mm) denoted by 'h', the average thickness of per layer deposited weld metal (mm) denoted by 'a' in the above equation.

2. Experiment

AISI 304LN austenitic stainless steel pipe having 25 mm thickness and 300 mm inner diameter was used for the present investigation. The chemical composition investigated by the spectroscopy testing machine is shown in table 1. The spectroscopy test was done at five different location and an average value was calculated.

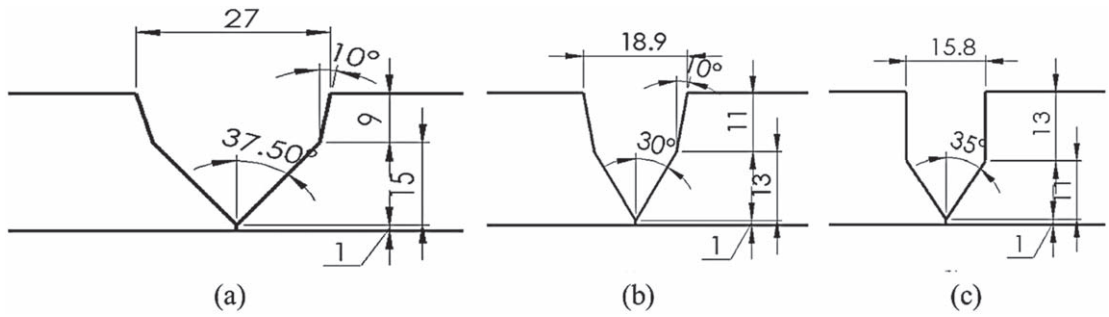

Figure 2. (a) Conventional groove (b) Narrow groove width 18.9 mm (b) Narrow Groove width 15.8 mm.

Table 2. Weld area of different groove geometry.

Name of groove and groove width	Weld area (mm^2)
conventional groove, 27 mm	398.10
narrow groove, 18.9 mm	288.84
narrow groove, 15.8 mm	283.60

Table 3. GTAW parameter for root pass.

Voltage (V)	Current(A)	Welding speed (cm min^{-1})
14	185	5.0–7.6

The consumables used for GMAW was filler wire/electrode and shielding gas. For GMAW process commercial argon of 99.98% purity was used as a shielding gas. The filler wire/electrode was selected as per the WRC-92 Siewert diagram [5, 7] to avoid hot cracking. SFA-5.9-ER308L filler wire was used for welding with a 1.2 mm diameter of the electrode. A modern transistorized power source of EWM make, Phoenix 401 Concept plus FKG/Phoenix, 401 Concept plus FKW model was used. During P-GMAW welding wire feed rate was capable of self-adjusting the other parameters such as arc voltage, peak current, background current, or base current.

A 1G position control fixture unit to control the rotation of pipe with the help of dc motor to give continuous rotation and position of pipe was used. The pipe was clamped on the fixture plate with the help of four slot fixture. The plate can handle pipe range 150 mm to 900 mm outer diameter. Torch manipulator is used to holding the torch at a given angle and distance. It has five degrees of freedom. It has an arm that can move up-down and left-right. A gun fixture is mounted on this arm, rotating and giving small movement in up-down and left-right direction.

ASME section ix as per boiler and pressure code was used for Conventional and narrow groove designing [16]. The conventional groove has an angle of attack between 35° to 45°. There are some parameters, which should be kept in mind while designing a narrow groove. These parameters include groove width, angle of attack, depth of fusion and electrode to work distance. With this consideration three different grooves are designed having groove width of 27.0 mm (Conventional groove), 18.9 mm and 15.8 mm (narrow groove) as shown in figure 2. By changing the groove design, will change the weld area that to be filled by welding process. The conventional groove area is 398.10 mm^2, which is 40% higher as compare to narrow groove as shown in table 2.

Root pass of all grooves was done by GTAW process and the process parameters are shown in table 3. The GMAW process parameter study was done on conventional and narrow groove welding and selected based on weld bead height, width, penetration, and weld pass on the groove. A typical appearance of the first and ninth weld pass on the conventional groove is shown in figure (a). The first and fifth weld pass on the narrow groove is shown in figures 3(a), (b), the final parameter for the GMAW welding on conventional and narrow grooves, as shown in table 4. Heat input per unit length has been calculated by equation no (i) and (ii) for GMAW and P-GMAW process, respectively, where arc efficiency (η) was considered as 0.7 [17].

$$\text{Heat input } (KJ/\text{cm}) = \eta \times \frac{Welding\ Current\,(A) \times Arc\ Voltage\,(V)}{1000 \times Welding\ speed\ (\text{cm}/s)} \quad \text{(i)}$$

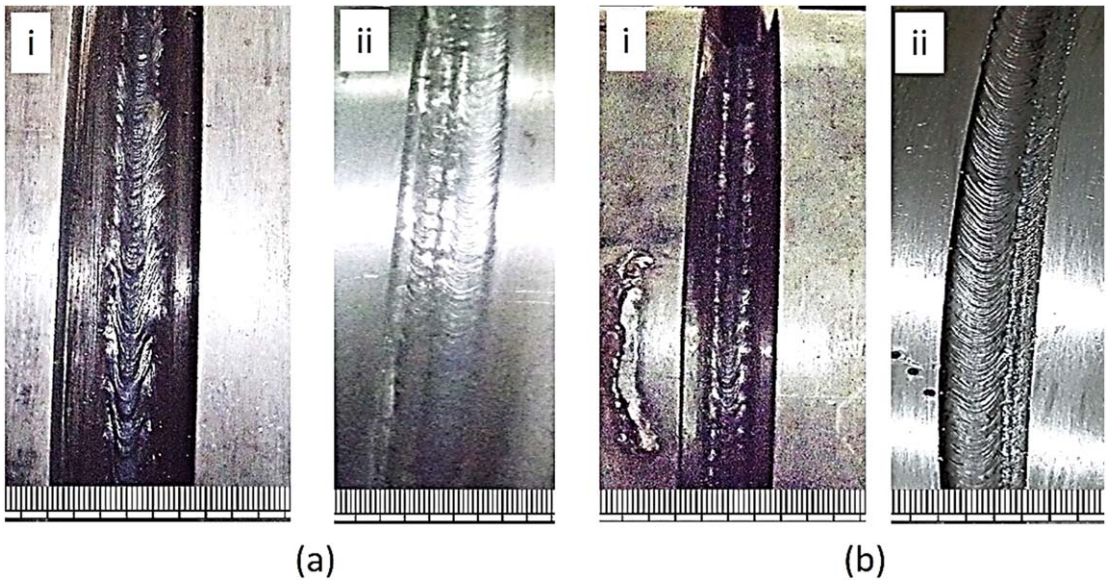

Figure 3. At a given heat input, the typical appearance of bead on (a) conventional groove at different weld pass (i) 1st weld pass (ii) 9th weld pass (b) narrow groove at (i) 1st weld pass (ii) 5th weld pass.

Table 4. Welding parameters for conventional and narrow groove.

Welding process	Groove	Voltage (V)	Gas flow rate l min^{-1}	Travel speed S cm min^{-1}	Welding parameters I/I$_m$	Welding parameters I$_p$ I$_b$ t$_b$ t$_p$ (A)(A) (s) (s)	Heat input (kJ cm^{-1})
GMAW	Conventional (27 mm)	27.2 ± 1.5	10	19.8	230	—	12.85 ± 0.53
P-GMAW	Conventional(27 mm)	24.1 ± 1.5	14	13.3	140	210 70 .2 .2	11.22 ± 0.35
P-GMAW	Narrow groove (18.9 & 15.8)	23.2 ± 1.5	14	13.3	135	200 70 .2 .2	10.07 ± 1.25

$$\text{Heat input (KJ/cm)} = \eta \times \frac{\text{Mean Current(A)} \times \text{Arc Voltage(V)}}{1000 \times \text{Welding speed(cm/s)}} \quad \text{(ii)}$$

Where,

$$\text{Mean Current(A)} = \frac{(I_p \times t_p) + (I_b \times t_b)}{t_p + t_b}$$ I_p is Peak current, I_b is base current, t_p is Peak current time and t_b is Base current time

The tensile test was performed as per the ASTM E8M specification. The tensile test was performed on at least three specimens to conclude the average final tensile property. The dimension of the tensile sample was shown in figure 4, and the cutting location of the sample shown in figure 5.

Impact toughness test of the base material and weld centre was carried out at ambient temperature by Charpy V-notch. Square cross-sectioned (10 × 10 mm) specimen according to the ASTM E23 specification was used for the test. The base material specimen with notch location at circumferential and transverse direction, as shown schematically in figure 5 was tested. The notch was located in the circumferential direction of the weld centre therefore the cracking plane lies along the direction of welding.

Vicker hardness tester was used to find the hardness of base metal, weld joint across the weld and HAZ. 5 kg load with 30 s dwell time was used to make an indentation and find the properties. The test was carried out at the centre line, 5 mm away from the centreline in weldment, HAZ and base metal.

One method to check the uniformity of weld without the specimen's destruction is ultrasonic inspection. The basic principle behind this test is the loss of energy of the high-frequency waves sent in the weld. When it encounters any discontinuity, it shows some attendant loss. During this process, the subsurface defect is detected

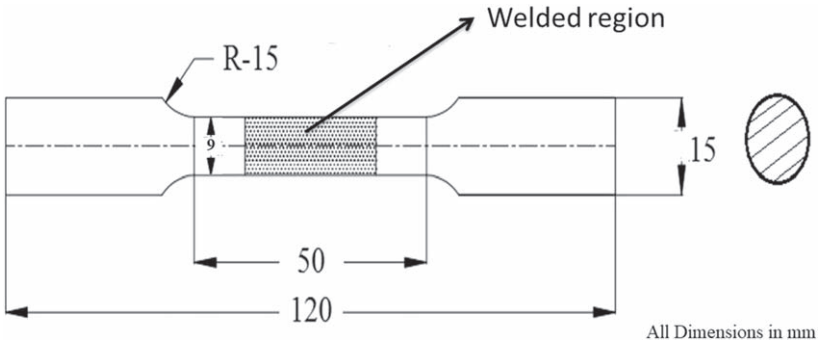

Figure 4. Tensile test specimen diagram.

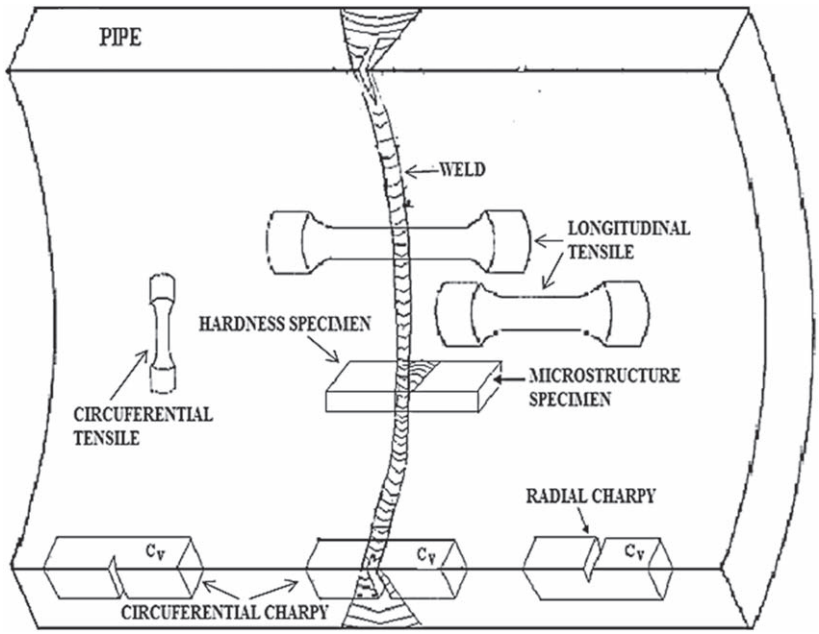

Figure 5. Schematic view for the collection of specimens from various locations in the weld and base metal for different mechanical testing.

without any damage to the material. The meanwhile display shows the reflected beam, which is then analysed to find the defect spot and its location.

There are two axes on-screen X (horizontal) and Y (vertical). The *X*-axis shows the depth of discontinuities, and *Y*-axis shows the intensity of discontinuities. The ultrasonic test result shows no peaks in the weld region; hence weld was qualified as a sound weld. Ultrasonic inspection has some advantages such as high sensitivity for planer defect, and results are received immediately, higher accuracy to find the position, size, shape and nature of the defect, size and weight of the machine is less, so it is easy to portable, high penetration capability and requires only one flat surface to do the test.

3. Result and discussion

The macroscopic cross-section view of the weld bead of GMAW and P-GMAW process on conventional and narrow grooves has been shown in figure 6. Figure 6 depicts there is no flaw and the weld was sound and free from any defect. The conventional groove consist of 11 weld passes for GMAW and P-GMAW process, whereas the narrow groove has eight weld passes. The groove's total heat input is 140, 115, 82 kJ cm^{-1} for conventional groove GMAW process, conventional groove P-GMAW process, and Narrow groove P-GMAW process, respectively.

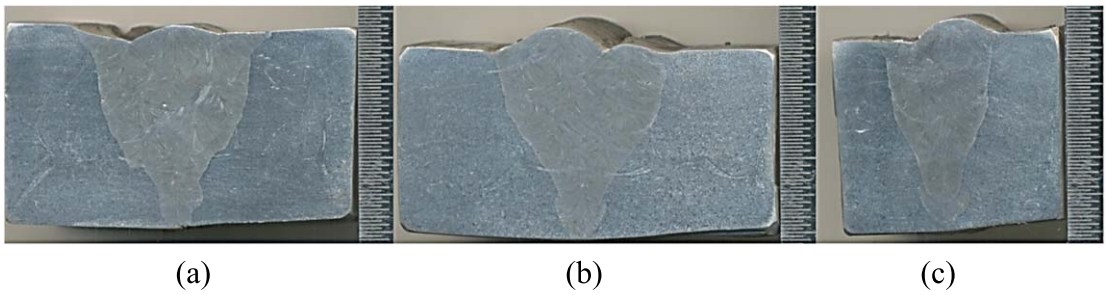

Figure 6. (a) Conventional groove welded by GMAW, (b) conventional groove welded by P-GMAW, (c) narrow groove welded by P-GMAW.

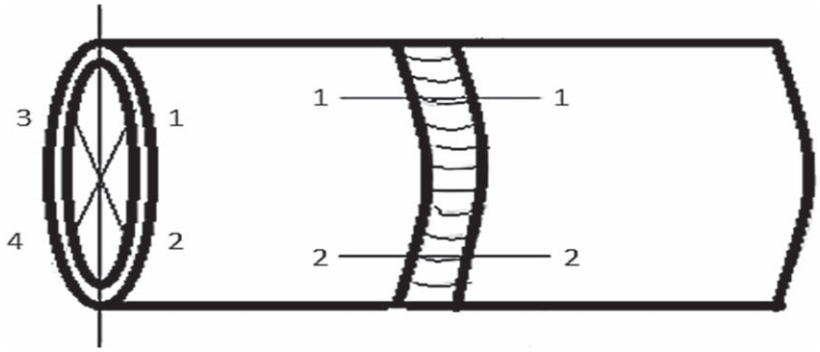

Figure 7. Schematic of circumferential locations to measure shrinkage.

Table 5. Cumulative Transverse shrinkage for conventional pipe weld joints.

Process	Groove type	Heat input (kJ cm^{-1})	No. of pass	Cumulative shrinkage in the pipe, (mm)				Average shrinkage (mm)
				1–1	2–2	3–3	4–4	
GMAW	Conventional (27 mm)	12.85 ± 0.53	11	5.11	5.28	6.05	5.78	5.56
P-GMAW	Conventional (27 mm)	11.22 ± 0.35	11	4.70	4.31	4.11	4.63	4.44

Table 6. Cumulative transverse shrinkage for pipe weld joints.

Process	Groove type (groove width in mm)	Heat input (kJ cm^{-1})	No. of pass	Cumulative shrinkage in the pipe, (mm)				Average shrinkage (mm)
				1–1	2–2	3–3	4–4	
P-GMAW	Narrow (18.9 mm)	10.07 ± 1.25	8	3.09	3.18	3.05	3.15	3.12
P-GMAW	Narrow (15.8 mm)	10.07 ± 1.25	8	2.76	2.95	2.82	2.85	2.85

3.1. Transverse shrinkage

The transverse shrinkage was measured after a subsequent weld pass. It was estimated by taking the distance between two points marked in the weld transverse direction. Initially, the distance was 50 mm after every pass we measure this distance. Reading was taken at four points which are marked on the circumference of pipe at equal distance.

Transverse shrinkage was measured at four different cross-sections of pipe, as shown in figure 7. The average cumulative transverse shrinkages on these cross-sections are shown in tables 5 and 6 for the conventional groove (weld by GMAW and P-GMAW) and narrow groove (weld by P-GMAW) process, respectively. The figure 8 depicts that the pipe of conventional groove welded by GMAW has the overall average shrinkage in the range of

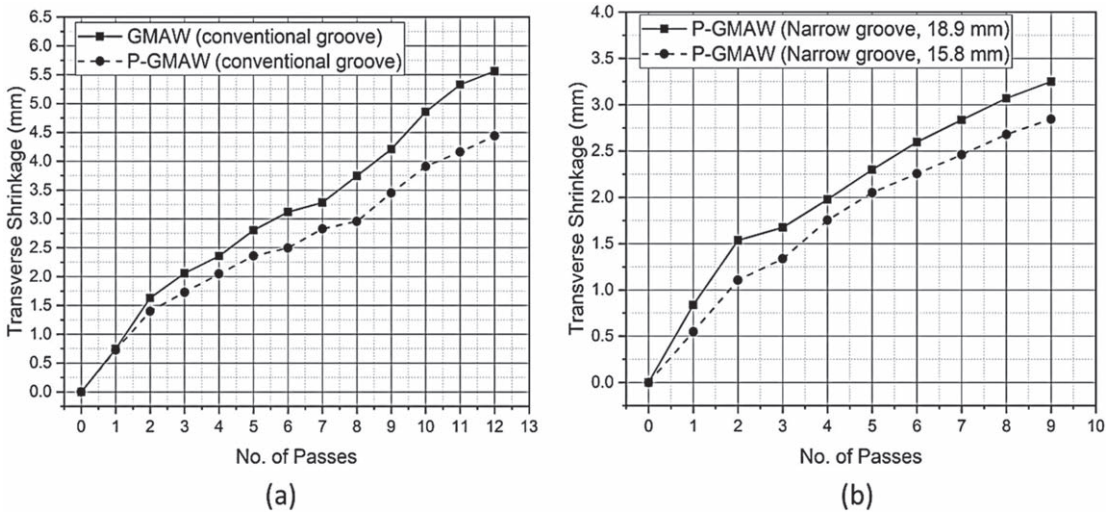

Figure 8. Average transverse shrinkage between subsequent passes (a) conventional grooves (b) Narrow groove weld.

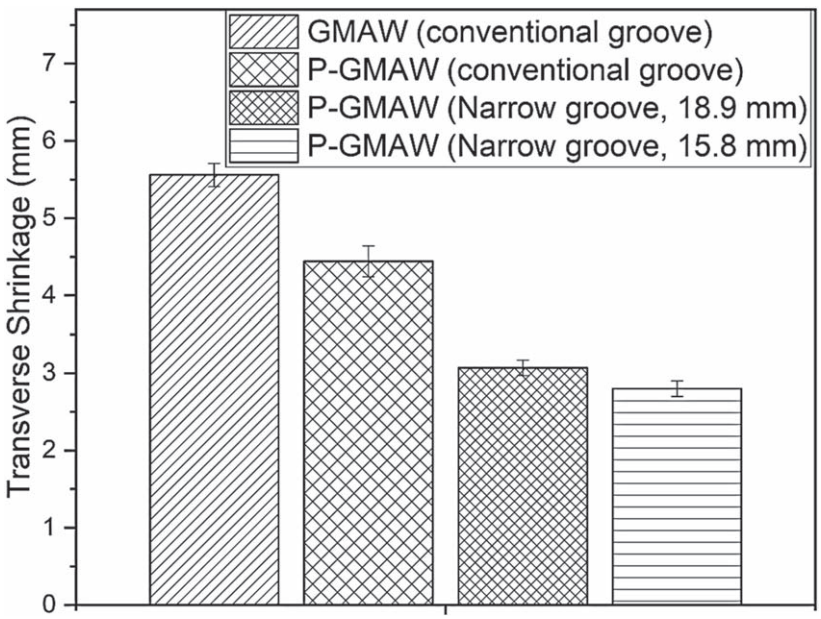

Figure 9. Average cumulative transverse shrinkage for all welds.

5.56 mm, which is approximately 1.16 mm higher than the pipe welded by the P-GMAW process in the same groove. This is happening because more heat is supplied in the GMAW process as compare to the P-GMAW process [18]. Further reduction in shrinkage was observed in the case of narrow groove pipe welded by the P-GMAW process. An approximate 45% reduction was observed in the shrinkage of narrow groove pipe weld by the P-GMAW process, as shown in figure 9, mainly due to a decrease in heat input and groove area. The figure 9 also depicts that the shrinkage will further increase as increase in the groove area.

3.2. Transverse shrinkage stresses

The estimation of transverse shrinkage stress is generally a function of heat input, weld area and plate thickness. The welding process is associated with a thermal cycle of heating and cooling rate of the weld pool; this is the primary reason for the development of transverse shrinkage. The equation no. (iii) is used for the measurement of transverse shrinkage stress [19].

Average transverse shrinkage stress (σ_{avg}) and standard deviation of welded pipe were calculate by using equation no (iv).

Table 7. Estimated value of $\sigma_{(i-i)}$ and $\sigma_{(i-j)}$ for the conventional groove weld prepared using GMAW process.

Estimated value of $\sigma_{(i-i)}$ (MPa)	Estimated value of $\sigma_{(i-j)}$ (MPa)
$\sigma_{(1-1)} = \frac{5.11}{11} \times \frac{3.56}{25} \times \frac{200 \times 1000}{50} = 264.83$	$\sigma_{(1-2)} = (\sigma_{(1-1)} + \sigma_{(2-2)})/2$ $= (264.83 + 280.32)/2$ $= 272.58$
$\sigma_{(2-2)} = \frac{5.28}{11} \times \frac{3.65}{25} \times \frac{200 \times 1000}{50} = 280.32$	$\sigma_{(2-3)} = (\sigma_{(2-2)} + \sigma_{(3-3)})/2$ $= (280.32 + 325.60)/2$ $= 302.96$
$\sigma_{(3-3)} = \frac{6.05}{11} \times \frac{3.75}{25} \times \frac{200 \times 1000}{50} = 325.60$	$\sigma_{(3-4)} = (\sigma_{(3-3)} + \sigma_{(4-4)})/2$ $= (325.60 + 300.14)/2$ $= 312.87$
$\sigma_{(4-4)} = \frac{5.78}{11} \times \frac{3.57}{25} \times \frac{200 \times 1000}{50} = 300.14$	$\sigma_{(4-1)} = (\sigma_{(4-4)} + \sigma_{(1-1)})/2$ $= (300.14 + 264.83)/2$ $= 282.49$
Estimation of the $\sigma_{avg} = \frac{1}{4} \times (272.58 + 302.96 + 312.87 + 282.87) = 292.82$	
Estimation of S.D. $= \sqrt{\left[\frac{1}{4} \times \{(292.82-272.58)^2 + (292.82-302.96)^2 + (292.82-312.87)^2 + (292.82-282.87)^2\}\right]} = 14.45$	

Table 8. Transverse stresses showing its nature at different locations of conventional (27 mm) groove welded by GMAW.

Weld location	Transverse shrinkage stress (MPa)	Nature	Average transverse shrinkage stress ± Std. Dev. (MPa)
1–2	272.58	Compressive	
2–3	302.96	Tensile	
3–4	312.87	Tensile	292.82 ± 14.45
4–1	282.87	Compressive	

Table 9. Transverse stresses showing its nature at different locations of conventional (27 mm) groove welded by GMAW.

Weld location	Transverse shrinkage stress (MPa)	Nature	Average transverse shrinkage stress ± Std. Dev. (MPa)
1–2	238.37	Tensile	
2–3	218.61	Compressive	
3–4	229.62	Compressive	234.00 ± 11.31
4–1	249.38	Tensile	

$$\sigma_{avg} = \sum_{i=0}^{4} \frac{\sigma_{tr(i-j)}}{4} \quad \text{(iii)}$$

$$\text{standard deviation (S.D.)} = \sqrt{\frac{1}{4} \times \sum_{i=0}^{4} (\sigma_{avg} - \sigma_{avg})^2} \quad \text{(iv)}$$

The transverse shrinkage stresses in a different cross-section (as shown in figure 7) are shown in table 7 for conventional groove welded by GMAW process, which shows the maximum stress of 325 MPa in pipe cross-section 3-3. The stress in intermediate pipe cross-section 1-2 and 4-1 are in compressive nature, and the other cross-section has tensile nature of the stress based on the increasing or decreasing nature of the stress. The stresses were reduced by 20% when the same groove welded by the P-GMAW process, as shown in table 8. This is happening due to the reduction of the cooling rate from 12.85 ± 0.53 kJ cm^{-1} to 11.22 ± 0.35 kJ cm^{-1} by the application of the P-GMAW process are shown in table 9. Further, reduction in groove area and heat input per pass as a narrow groove and their stresses are shown in tables 10 and 11 for the narrow groove 18.9 and 15.8 mm, respectively. These result shows further reduction in the stress to 214.32 ± 8.40 MPa for 18.9 mm narrow groove and 202.80 ± 9.48 MPa for 15.8 mm narrow groove.

3.3. Microstructure

The typical weld microstructures of base metal is shown in figure 10. The weld microstructures for a given heat input of 12.85 ± 53 kJ cm^{-1} using GMAW process is shown in figures 11(a) and (b) respectively. Similarly, for P-GMAW at a given heat input for conventional groove 11.22 ± 0.35 kJ cm^{-1} and narrow groove 9.25 ± 1.5 kJ cm^{-1}, the typical microstructures of weld deposits have been shown in figures 11(c)–(f) respectively. The microstructures presented in figure 11 shows different morphology for P-GMA and GMA welds depending on their multipass weld deposits. The P-GMA weld deposit shows considerable refinement in microstructure along

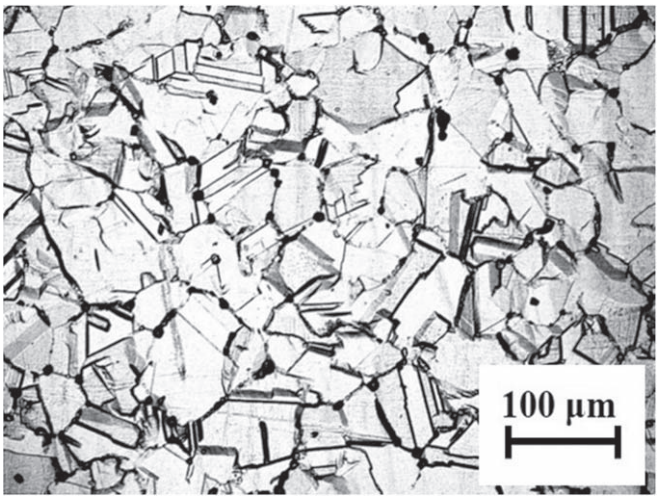

Figure 10. Typical microstructure of base metal.

Table 10. Transverse stresses showing its nature at different locations of narrow (18.9 mm) groove welded by GMAW.

Weld location	Transverse shrinkage stress (MPa)	Nature	Average transverse shrinkage stress ± Std. Dev. (MPa)
1–2	224.80	Tensile	214.32 ± 8.40
2–3	210.36	Compressive	
3–4	202.86	Compressive	
4–1	219.29	Tensile	

Table 11. Transverse stresses showing its nature at different locations of narrow (15.8 mm) groove welded by GMAW.

Weld location	Transverse shrinkage stress (MPa)	Nature	Average transverse shrinkage stress ± Std. Dev. (MPa)
1–2	194.73	Compressive	202.80 ± 9.48
2–3	209.87	Tensile	
3–4	214.30	Tensile	
4–1	192.19	Compressive	

with scarcely distributed coaxial dendritic structure, whereas the GMA welds significantly consists of both coaxial dendritic and reheated refined regions [20]. In P-GMA welds, the increased grain refinement in microstructure was observed with the lowering of heat input from 11.22 to 9.25 kJ cm^{-1} respectively (figure 11).

The typical microstructures of the HAZ of the conventional weld joint prepared at a given heat input of 11.22 ± 1.35 kJ cm^{-1} by using the P-GMAW process have been shown in figures 11(c) and (d) respectively. Similarly, at a given heat input of 9.25 ± 1.5 kJ cm^{-1}, the typical microstructures of weld HAZ shown in figures 11(e) and (f) respectively. Coarse grained microstructure was observed at the HAZ adjacent to the fusion line of the P-GMA, GMA weld [20].

3.4. Mechanical properties

3.4.1. Tensile properties

The comparative analysis of tensile properties for GMAW and P-GMAW weld joints of the pipes are shown in figure 12. The base material having an ultimate tensile strength of 532 MPa and yield strength of 265 MPa. The figure 11 depicts that the tensile properties of welded pipe are more in all conditions than the base material. The conventional groove welded by the GMAW process achieves a yield strength of 280 MPa and ultimate strength of 548 MPa, Which P-GMAW can increase because the P-GMAW process has a pulsing arc. The maximum yield strength and ultimate strength was observed as 320 MPa and 574 MPa respectively, when the pipe was welded by the P-GMAW process for the narrow groove of 15.8 mm. As heat input increases due to arcing parameter or groove area increases, there is a significant reduction in yield strength but ultimate strength remains more or less the same. This behaviour confirms the microstructural characteristics of the weld at different heat input [21, 22].

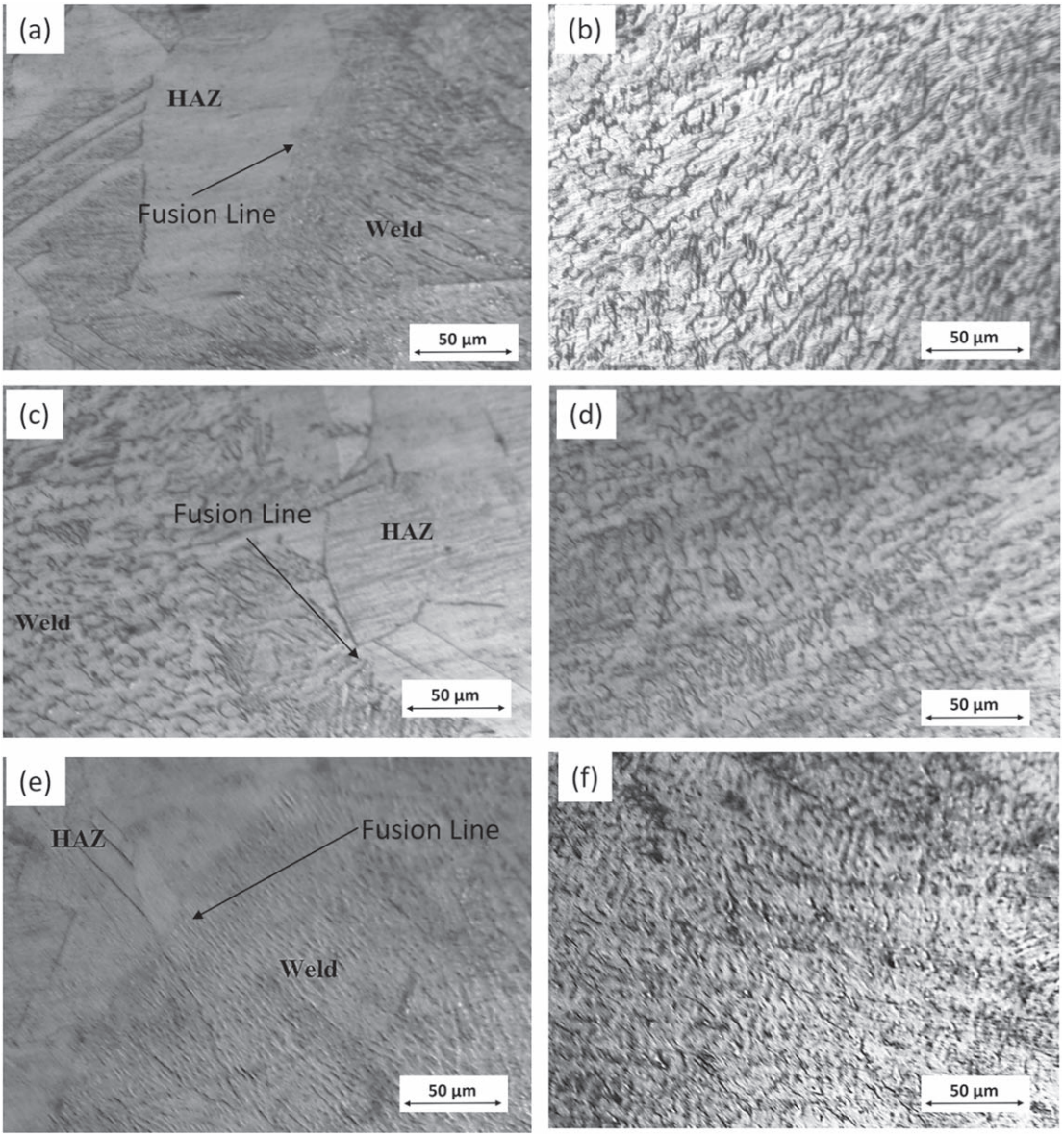

Figure 11. Typical microstructure (a) conventional groove (27 mm) at near fusion line (b) conventional groove (27 mm) in FZ, (c) P-GMA weld conventional groove (27 mm) at near fusion line (d) P-GMA weld conventional groove (27 mm) in FZ, (e) P-GMA weld narrow groove (18.9 mm) at near fusion line (f) P-GMA weld narrow groove (18.9 mm) in FZ.

In P-GMA welds, the tensile properties improve with the lowering of heat transfer in the longitudinal directions due to the almost similar chemical composition of weld deposits with the variation in pulse parameters.

3.4.2. Charpy impact toughness

Charpy impact energy test was performed at room temperature (RT) for all weld joints having notch orientation in their circumferential direction (figure 5). A set of fracture samples has been shown in figure 13 and the result has been given in table 12. The table primarily depicts that all the weld joints have passed the acceptance criterion (minimum value of 120 J for Charpy impact toughness in base metal and 90 J in the weld metal [23]. Such improvement in fracture toughness is primarily governed by refinement in microstructure in the weld zone [24]. The P-GMAW process shows more refinement in the matrix as compared to the GMAW process because of the pulsing effect of arc as discussed in the microstructure.

3.4.3. Hardness

The location of the hardness test has been shown in figure 14, where CL is the centre line and FL is the fusion line. The influence of variation on hardness in P-GMA and GMA welds in transverse and through weld has been shown in figure 15. A maximum hardness of 270 HV at CL was observed in narrow groove welded by the

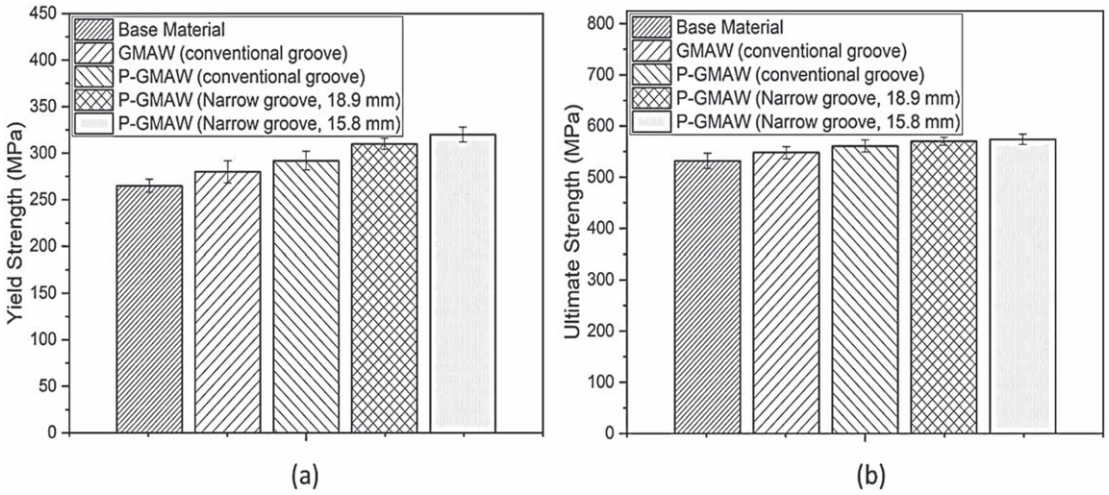

Figure 12. Tensile properties for GMA and P-GMA weld joints of different grooves at their circumferential direction.

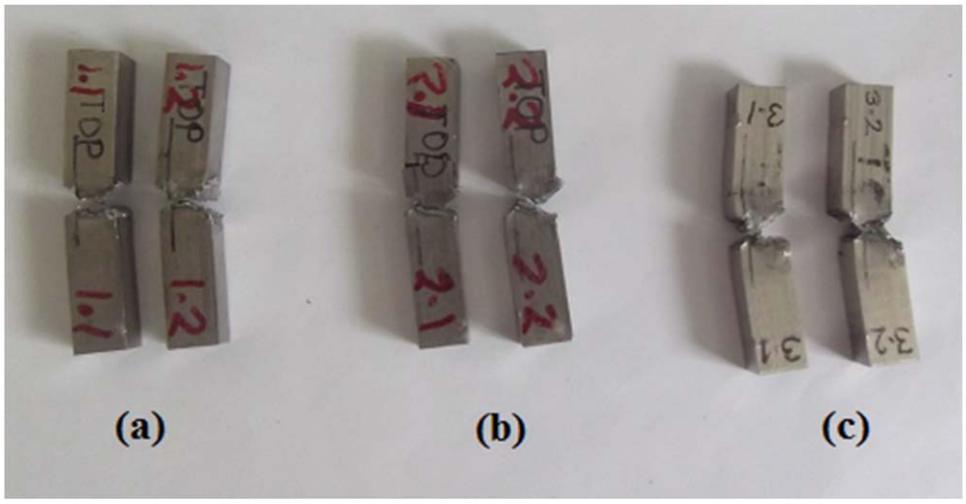

Figure 13. Photograph showing the Charpy specimen after weld test (a) GMA weld, conventional groove, (b) P-GMAW, conventional, (C) P-GMAW, narrow (18.9 mm) groove.

Table 12. Charpy properties for GMA and P-GMA weld joints of different grooves at their circumferential direction.

Process	Groove width (mm)	Heat input (KJ cm^{-1})	Energy absorbed, (J)	
GMAW	27	12.85 ± 0.53	136	143
			143	
			150	
P-GMAW	27	11.22 ± 0.35	135	147.5
			145	
			162	
	18.9	10.07 ± 1.25	155	160
			155	
			170	
	18.9	10.07 ± 1.25	154	160
			159	
			168	

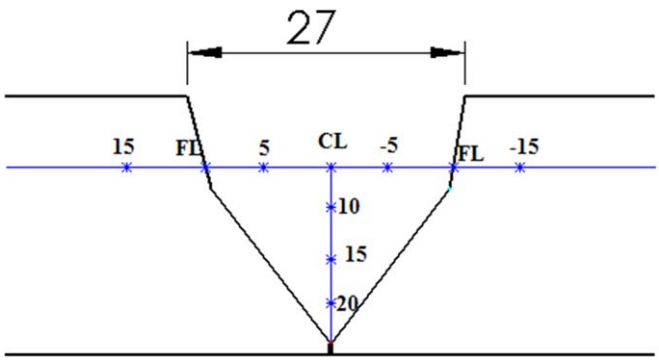

Figure 14. Schematic representation of different points where hardness was taken.

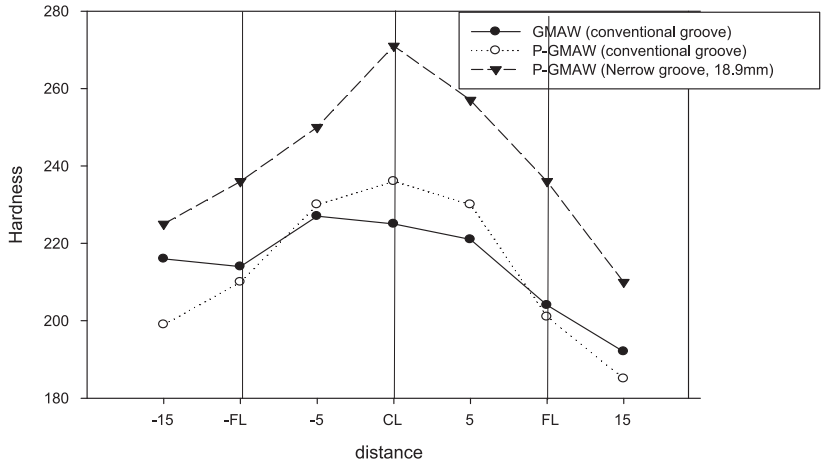

Figure 15. The typical variation in hardness observed across the width of the GMA and P-GMA weld in conventional and narrow grooves.

P-GMAW process at heat input of 10.07 $\pm$ 1.25 kJ cm^{-1} compared to the other joint at heat input of 12.85 $\pm$ 0.53 kJ cm^{-1}, which gives a clear avoidance of high cooling rate in the weld zone. Further, The variation in microstructure may have affected the hardness distribution in weld deposits due to its influence on the size and distribution of carbide precipitation [25] in the matrix. Hardness distribution in weld deposit and HAZ for conventional groove GMAW weld joint at heat input of 12.85 $\pm$ 0.53 kJ cm^{-1} is relatively lower than conventional and narrow groove welded by P-GMAW at heat input of 10.07 $\pm$ 1.25 kJ cm^{-1}.

4. Conclusion

- P-GMA welding produced sound weld over conventional groove GMA at a comparatively lower heat input of 11.22 $\pm$ 1.35 KJ cm^{-1}. Reduced transverse shrinkage and comparatively lower weld shrinkage stress was observed in P-GMA welding over GMA welding.
- Narrow groove welding using P-GMAW process resulted in reduction in number of passes and area of weld deposit to about 30%–40% by volume.
- Narrow groove design using P-GMAW process reduced shrinkage stresses at almost constant heat input.
- Tensile properties were improved by 5%–10% by using P-GMA welding process.
- Narrow groove design having lower weld deposited area ensued lower heat input that led to decreased transverse shrinkage and lowering shrinkage stress to 20%–35%.
- The major observation was that the Narrow groove design with P-GMAW process can remarkably minimize the transverse shrinkage and shrinkage stresses of the weld.

Data availability statement

All data that support the findings of this study are included within the article (and any supplementary files).

ORCID iDs

Sudhir Kumar https://orcid.org/0000-0002-7862-6236

References

[1] Padilha A F and Rios P R 2002 Decomposition of austenite in austenitic stainless steels *ISIJ Int.* **42** 325–37
[2] Covert R A and Tuthill A H 2000 Stainless steels: an introduction to their metallurgy and corrosion resistance *Dairy, Food and Environmental Sanitation* **20** 506–17
[3] Folkhard E 1984 *Welding Metallurgy of Stainless Steels* (Wien: Springer)
[4] Kearns L P *et al* 1978 *Welding Handbook* II (Miami, FL: American Welding Society) 131–7
[5] ASM handbook 1994 *Welding, Brazing and Soldering* 6 (Russell Township, Geauga County, OH: ASM International) Materials Park, OH
[6] S´anchez-Cabrera V M, Rubio-Gonz´alez C, Ru´ız-Velab J I and Ram´ırez-Baltazar C 2007 Effect of preheating temperature and filler metal type on the microstructure, fracture toughness and fatigue crack growth of stainless steel welded joints *Mater. Sci. Eng., A* **452–453** 235–43
[7] Tujsek J 2000 Experimental investigation of gas tungsten arc welding and comparison with theoretical predictions *IEEE Trans. Plasma Sci.* **28** 1688–93
[8] Redding C J 2002 Fume model for gas metal arc welding *Welding Journal* **6** 95s–03s
[9] Ghosh P K 1996 An analysis of weld characteristics as a function of pulse current MIG welding parameters *International Journal on Joining of Materials* **8** 157–61
[10] Allum C J and Quintino L 1985b Control of fusion characteristics in pulsed current MIG welding: II. Simple model of fusion characteristics *Metal Construction* **17** 314R –317R
[11] Amin M 1983 Pulse current parameters for arc stability and controlled metal transfer in arc welding *Metal Construction* **15** 272–87
[12] Kumar S and Ghosh P K 2018 TIG arc processing improves tensile and fatigue properties of surface modified of AISI 4340 steel *Int. J. Fatigue* **116** 306–16
[13] Kumar S, Ghosh P K and Kumar R 2017 Surface modification of AISI 4340 steel by multi-pass TIG arcing process *J. Mater. Process. Technol.* **249** 394–406
[14] Ghosh P K and Sharma V 1991 Weld bead chemistry and its characteristics in pulsed MIG welded Al–Zn–Mg alloy *Mater. Trans., JIM* **32** 145–50
[15] Ghosh P K, Gupta P C and Jain N K 1989 Studies on the properties of weld deposit at various pulse frequencies in MIG welding of Al–Zn–Mg alloy *Indian Welding Journal* **68** 550–8
[16] Barla N A, Ghosh P K, Kumar V, Paraye N K, Anant R and Das S 2021 Simulated stress induced sensitization of HAZ in multipass weld of 304LN austenitic stainless steel *J. Manuf. Processes* **62** 784–96
[17] Ghosh P K, Gupta P C and Somani R 1991b Influence of pulse parameters on the porosity formation in pulsed MIG weld deposit of aluminium alloy *International Journal of Joining of Materials* **3** 49–54
[18] Kulkarni S, Rajamurugan G and Ghosh P K 2021 Prominence of narrow groove on pulsed current GMA and SMA welding of thick wall austenitic stainless steel pipe *Trans. Indian Inst. Met.* **74** 2297–312
[19] Pandey C, Narang H K and Saini N 2017 Microstructure and transverse shrinkage stress analysis in GTA welds of P91 steel pipe *Int. J. Steel. Struct.* **17** 763–74
[20] Ghosh P K, Gupta P C and Somani R 1991a Influence of pulse parameters on bead geometry and HAZ during bead on plate deposition by MIG welding process *Z. Metallkde.* **82** 756–62
[21] Kulkarni S G and Ghosh P K 2008 Improvement of weld characteristics by variation in welding processes and parameter in joining of thick wall 304LN stainless steel pipe *ISIJ Int.* **48** 1560–9
[22] Kumar R, Ghosh P K and Kumar S 2017 Thermal and metallurgical characteristics of surface modification of AISI 8620 steel produced by TIG arcing process *J. Mater. Process. Technol.* **240** 420–31
[23] Kumar S and Ghosh P K 2020 Thermal behaviour of TIG arc surfacing affecting mechanical properties of AISI 4340 steel substrate under static and dynamic loading *Mater. Sci. Eng. A* **773** 138734
[24] David S A, Vitek J M, Keiser J R and Oliver W C 1987 Use of a mechanical properties microprobe in the study of weld transformations *Metall. Trans. A* **18A** 1996–9
[25] Joseph A, Harwig D, Farson D F and Richardson R 2003 Measurement and calculation of arc power and heat transfer efficiency in pulsed gas metal arc welding *Sci. Technol. Weld. Joining* **8** 400–6